J. Indian Inst. Sci.
A Multidisciplinary Reviews Journal
ISSN: 0970-4140 Coden-JIISAD

REVIEW ARTICLE

Crystallography as a Path-Finding Tool to Understand Functionality in Coordination Polymers

*Dilip Kumar Maity and Debajyoti Ghoshal**

Abstract | Because of their potential applications, coordination polymers (CPs) are at an exalted position in the field of chemical and material science. Porous coordination polymers, popularly known as metal–organic frameworks (MOFs), have large surface area with functional pore environment, permanent porosity, tailorability in pore size, dimension and volume, which make them promising for interesting functionalities. In this review, we show how the mixed-ligand CPs/MOFs are very important in tuning the functionality of such systems and how the X-ray structure illuminates their functionalities. Here, we discuss the application of mixed-ligand functional MOFs for CO_2 storage and separation by fine-tuning their pore size and dimension along with their polar pore surfaces using different functional dicarboxylates and *N,N′*-donor ligands. We also discuss the nature of conductivity and fabrication of Schottky barrier diode for CPs, where free organic ligands are in their pores. In addition, we also present the variation of their interesting chemical reactivity, e.g. framework-assisted in situ redox transformation.

1 Introduction

Several stalwarts[1] have pointed out the genesis of chemical crystallography and how the batten has been transferred from the physicist to the hand of chemists. It is a well-established reality that chemical crystallography started with a vision to get an insight into molecular structure. In course of time, with increased ease of collecting single-crystal X-ray data as well as their structure solution, chemical crystallography has almost turned into a characterisation tool for organic as well as the metal–organic structures until the emergence of a new field called crystal engineering.[2, 3] Now, description of crystal engineering is not within the scope of this review, but how its idea helped to create coordination polymers (CPs) to unravel their functionality[4–7] is discussed here. We also discuss how crystal structures have helped us in some new findings and new understanding to plan our research at Jadavpur University.

The design of functional CPs and/or metal–organic frameworks (MOFs)[8, 9] has become a very promising area of research among contemporary researchers over the last two decades. This is obviously due to the ease of structural modulation for getting the desired functionalities.[4–7] Functional CPs and/or MOFs[8, 9] have attracted the interest of synthetic chemist because of their potential applications such as in gas storage and separation,[10, 11] catalysis,[12] conductivity and[13] sensing.[14, 15] Currently, we are investigating the selective sorption of CO_2 in properly designed frameworks. We have also studied some conducting CPs and shown how they can be useful for making barrier diode-type devices. In addition, we have also investigated some framework-dependent redox transformations in the light of crystal structure of CPs. These are presented in later sections.

Department of Chemistry, Jadavpur University, Kolkata 700 032, India
**dghoshal@chemistry.jdvu.ac.in*

Springer IISc Press

2 Design of Frameworks for Selective CO_2 Uptake

Like others in the field of metal–organic frameworks, this topic has attracted our interest due to uncontrollable rise in atmospheric CO_2 level day by day throughout the world, largely due to the burning of fossil fuels. This rise in atmospheric CO_2 causes drastic climate change, leading to global warming. Thus to minimise such released CO_2, the only hope is to scavenge the released CO_2, as civilisation cannot sustain without energy and green energy is still a distant dream. In addition, selectivity is also essential as most flue gases contain large amount of N_2, and if the capturing materials adsorb non-detrimental N_2, instead of greenhouse CO_2 gas, the role of materials will not be understood. Although carbon capture and sequestration (CCS) techniques[16] using amine scrubbing[17] or membrane separation have been utilised widely for CO_2 capture, it has some inherent economic viability limitations too.[18] However, zeolite[19] or activated carbon-like solid adsorbents can surmount these drawbacks to a large extent, but they are not very ideal to achieve selective CO_2 storage and separation due to lack of regularity in structures. However, judiciously synthesised MOFs are very effective as not only do they have appreciably high gas uptake capacity, but also their structures have regular and tunable pore sizes, dimensions and pore volumes. Interestingly, their pore surfaces can be decorated and designed by careful choice and/or variation of organic ligands with different functional groups and enhanced CO_2 uptake capacity. Here, we discuss some important strategies for better CO_2 uptake: (1) modification of pore wall using functional groups in organic linkers, and (2) tuning of pore sizes and/or dimensions. MOFs are designed by combining metal and organic linkers. Thus, the introduction of different chemical environments in the linkers can change the environment of pore walls, and the control in the length of linkers can modify pore sizes.

2.1 Modification of Pore Wall Using Functional Group in Organic Linker

This is the most convenient way to tune the structures of MOFs for CO_2 uptake selectivity, as the variation in polar functional groups can easily generate versatile polar pore surfaces and environments in the MOFs. So, in the last few decades, contemporary researchers have focussed on the design of MOFs containing different polar functional groups aligned to the pore wall (Scheme 1) for these purposes, as CO_2 is a quadrupolar (-1.4×10^{-39} C m^2) molecule with a strong affinity to the polar pore rather than the non-polar H_2, N_2 or CH_4 gases. So, it is a better way to enhance CO_2 selectivity with modulating polar pore surfaces incorporating different polar functional groups in the structures of both the organic linkers during the period of framework design of MOFs. In this context, earlier works[20, 21] clearly show that polar functional groups have significant impact on selective CO_2 adsorption to a varied extent. Here, we discuss this crucial aspect for selective CO_2 uptake considering three examples of functional groups in three respective sections.

2.1.1 Amine Group-Decorated Pore Wall

Incorporation of Lewis basic polar amine group in the pore wall of MOFs is one of the

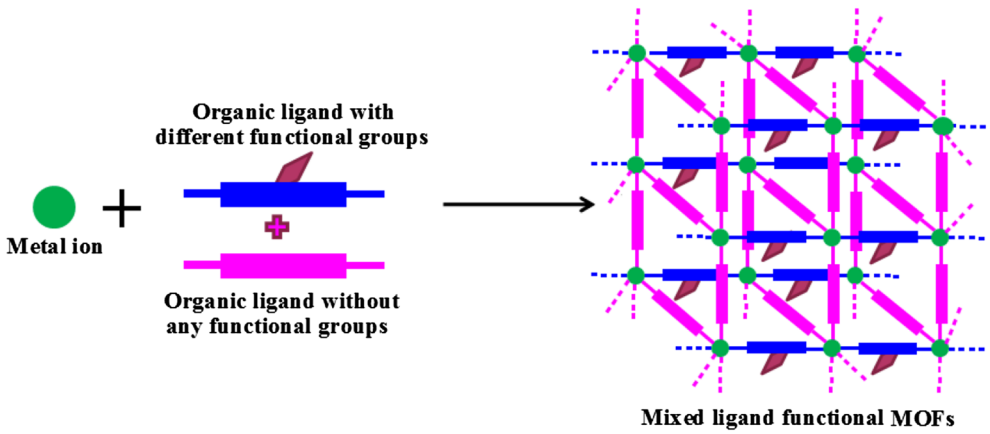

Scheme 1: Schematic representation for the synthesis of mixed ligand functional metal–organic frameworks (MOFs)

most promising techniques for selective CO_2 adsorption. Several groups[22–24] have studied the synthesis as well as functionality of amine group-functionalised MOFs extensively for selective CO_2 adsorption. It is clearly evident that the amine group is the best candidate for this than the other functional groups because of its smaller size and higher Lewis basicity. We have also mentioned about CO_2 molecule having quadrupole moment, where the C-atom is Lewis acidic in nature. So, simply considering Lewis acid–base interaction, amine group-functionalised MOFs can show greater CO_2 selectivity over other non-polar gases such as H_2, N_2 and CH_4. Some important examples[22–24] are discussed here.

Long et al. reported a water-stable, triazolate-bridged framework[22] of $H_3[(Cu_4Cl)_3(BTTri)_8]$ (H_3BTTri=1,3,5-tri(1H-1,2,3-triazol-4-yl) benzene) with incorporation of *N,N′*-dimethylethylenediamine (mmen) into the framework (Figure: 1a), which shows significantly enhanced CO_2 adsorption. At 25 °C and 1 bar, mmen–CuBTTri exhibits 4.2 mmol g^{-1} (15.4 wt%) of gravimetric CO_2 uptake (Figure: 1b), which is 15% greater than the gravimetric CO_2 uptake of unmodified CuBTTri. At 25 °C, under the mixture of 0.15 bar CO_2 and 0.75 bar N_2, mmen–CuBTTri exhibits 2.38 mmol g^{-1} (9.5 wt%) CO_2 uptake with a selectivity of 327, whereas the unmodified framework adsorbs only 0.69 mmol g^{-1} (2.9 wt%). Compound mmen–CuBTTri adsorbs less amount of N_2 gas than CuBTTri at all pressures between 0 and 1.1 bar (Figure: 1b) due to reduction in specific surface

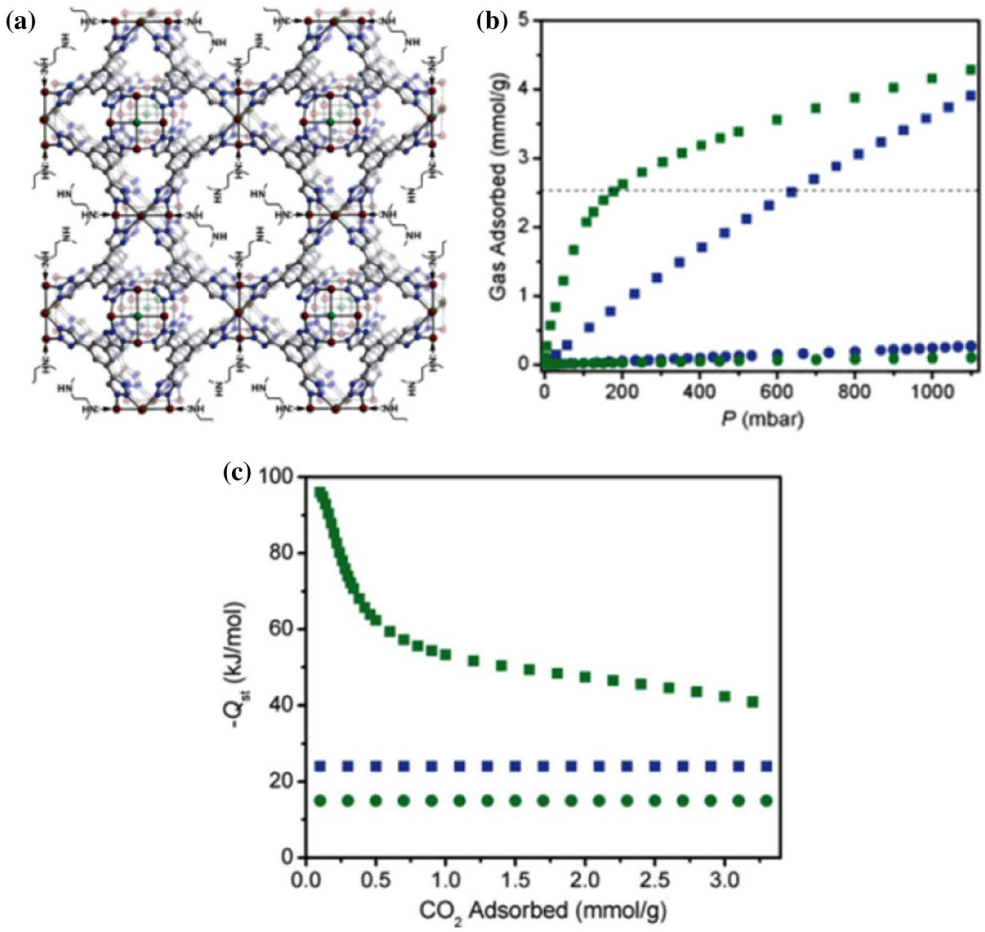

Figure 1: **a** Amine-functionalised metal–organic framework in mmen–CuBTTri; stoichiometric incorporation of the diamine *N,N′*-dimethylethylenediamine onto open metal sites in the pores. **b** Gravimetric adsorption of CO_2 (*squares*) and N_2 (*circles*) at 25 °C for mmen–CuBTTri (*green*) and CuBTTri (*blue*), respectively. **c** Isosteric heats of CO_2 adsorption for mmen–CuBTTri (*square green*) and CuBTTri (*square blue*). Reproduced with permission from Ref.[22] Copyright© 2011, Royal Society of Chemistry.

area with the incorporation of the mmen moiety. The exceptionally high CO_2 uptake capacity and selectivity for mmen–CuBTTri are the consequences of large isosteric heat of CO_2 adsorption (i.e. 96 kJ mol^{-1}) at zero coverage (Figure: 1c).

Maji et al. recently reported two Cd(II) MOFs,[23] $\{[Cd(NH_2\text{-bdc})(bpe)]\cdot 0.5EtOH\}_n$ and $\{[Cd(NO_2\text{-bdc})(azbpy)]\cdot 4H_2O\}_n$ (NH_2-bdc=2-amino terephthalic acid, bpe=1,2-bis(4-pyridyl)ethane, NO_2-bdc=2-nitro terephthalic acid, azbpy=4,4′-azobipyridine) and compared their selective CO_2 adsorption capacity over non-polar N_2 gas. Both the frameworks were constructed by exo-bidentate 4-pyridyl linkers of similar length, but with different functionalities. Compound $\{[Cd(NH_2\text{-bdc})(bpe)]\cdot 0.5EtOH\}_n$ exhibits an amine group-decorated 3D structure with 1D guest ethanol-filled channels (Figure: 2a, b). But, compound $\{[Cd(NO_2\text{-bdc})(azbpy)]\cdot 4H_2O\}_n$ has a twofold interpenetrated 3D framework structure, where large-sized pendant $-NO_2$ groups of NO_2-bdc are aligned to the pore surface (Figure: 2c). The dehydrated $\{[Cd(NH_2\text{-bdc})(bpe)]\cdot 0.5EtOH\}_n$ exhibits a selective type-I CO_2 uptake profile up to ~39 mL g^{-1} over N_2 at 195 K with a reasonably high isosteric heat of adsorption value (Figure: 2d). On the other hand, the dehydrated framework of $\{[Cd(NO_2\text{-bdc})(azbpy)]\cdot 4H_2O\}_n$ exhibits a comparatively lower CO_2 uptake up to 15 mL g^{-1} at 195 K than the previous one due to structural contraction and smaller pore dimension of the 1D channel.

In this context, our group also reported two amino-functionalised MOFs,[24] $\{[Zn(NH_2\text{-bdc})_2(4\text{-bpdb})]\cdot(H_2O)_4\}_n$ and $\{[Zn_2(NH_2\text{-bdc})(4\text{-bpdh})]\cdot(H_2O)_4\}_n$ (where 4-bpdb=4,4-bis-

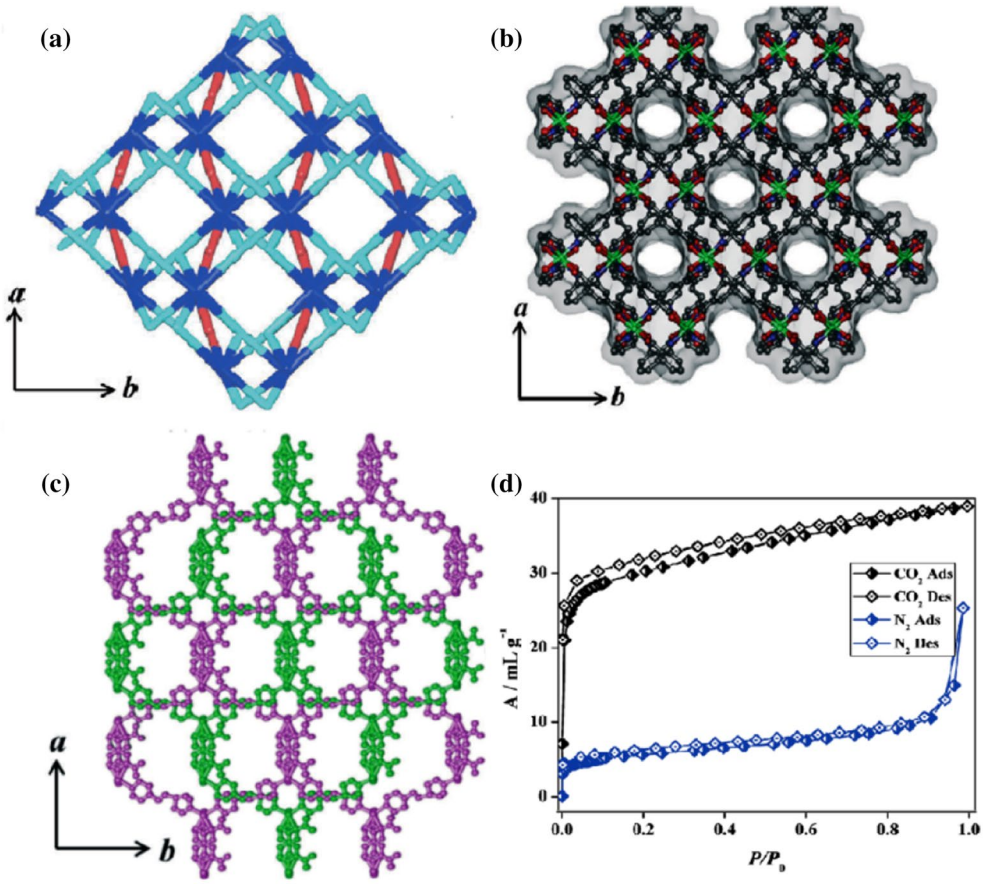

Figure 2: **a** A view of the 3D net in $\{[Cd(NH_2\text{-bdc})(bpe)]\cdot 0.5EtOH\}_n$ along the *c*-axis. **b** The distorted *square*-shaped pore along the *c*-axis in $\{[Cd(NH_2\text{-bdc})(bpe)]\cdot 0.5EtOH\}_n$. **c** A view of the twofold interpenetrated nets along the *c*-axis in $\{[Cd(NO_2\text{-bdc})(azbpy)]\cdot 4H_2O\}_n$. **d** N_2 (*blue*) and CO_2 (*black*) adsorption profiles of dehydrated $\{[Cd(NH_2\text{-bdc})(bpe)]\cdot 0.5EtOH\}_n$ at 77 and 195 K, respectively; *filled* and *open squares* signify the adsorption and desorption, respectively. Reproduced with permission from Ref.[23] Copyright© 2014, Royal Society of Chemistry.

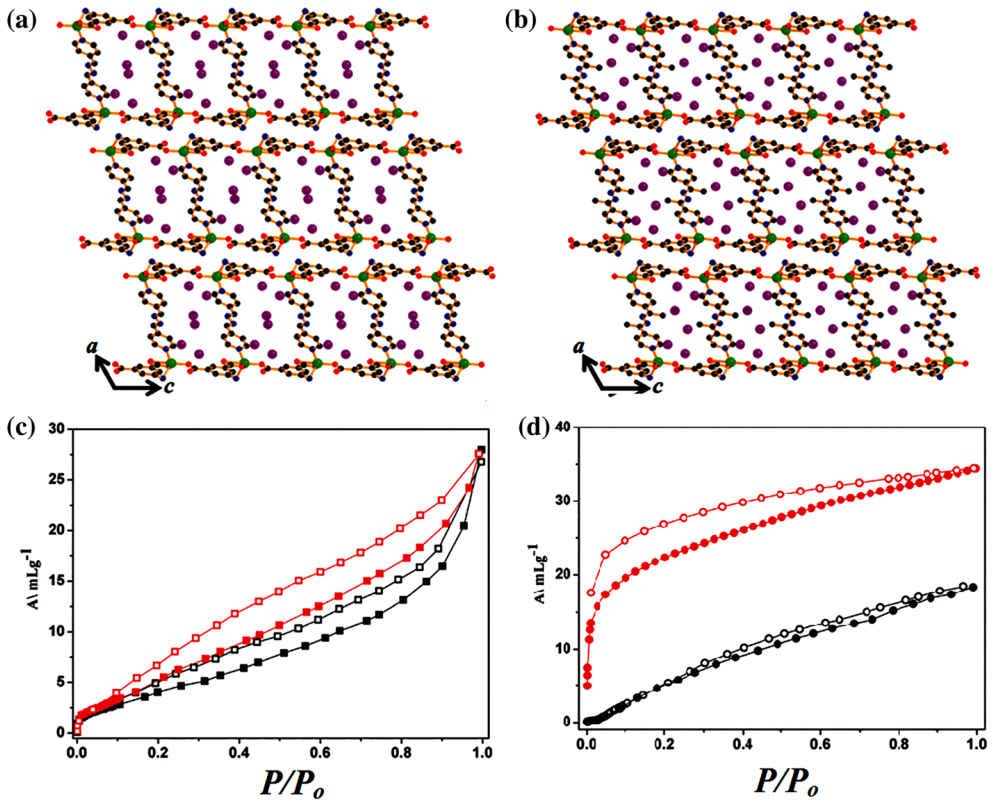

Figure 3: **a**, **b** 2D pillared-bilayer framework showing guest water-filled 1D channel viewed along the *b*-axis for compounds $\{[Zn(NH_2\text{-bdc})_2(4\text{-bpdb})]\cdot(H_2O)_4\}_n$ and $\{[Zn_2(NH_2\text{-bdc})(4\text{-bpdh})]\cdot(H_2O)_4\}_n$, respectively. **c** N_2 sorption isotherms for the dehydrated frameworks of $\{[Zn_2(NH_2\text{-bdc})(4\text{-bpdb})]\cdot(H_2O)_4\}_n$ (*red squares*) and $\{[Zn_2(NH_2\text{-bdc})(4\text{-bpdh})]\cdot(H_2O)_4\}_n$ (*black squares*) at 77 K, respectively: adsorption (*filled squares*); desorption (*open squares*). **d** CO_2 adsorption isotherms for the dehydrated frameworks of $\{[Zn(NH_2\text{-bdc})_2(4\text{-bpdb})]\cdot(H_2O)_4\}_n$ (*red circles*) and $\{[Zn_2(NH_2\text{-bdc})(4\text{-bpdh})]\cdot(H_2O)_4\}_n$ (*black circles*) at 195 K: adsorption (*filled circles*); desorption (*open circles*). Reproduced with permission from Ref.[24] Copyright© 2015, Royal Society of Chemistry.

(4-pyridyl-2,3-diaza-1,3-butadiene, 4-bpdh=2,5-bis-(4-pyridyl)-3,4-diaza-2,4-hexadiene and NH_2-bdc=5-amino-1,3-benzenedicarboxylate). Both the compounds exhibit two-dimensional (2D) pillared-bilayer framework (Figure: 3a, b) containing lattice water-filled 1D channels with dimensions of 8.3 × 3.8 $Å^2$ and 8.0 × 1.6 $Å^2$, respectively. The channel dimension of $\{[Zn_2(NH_2\text{-bdc})(4\text{-bpdh})]\cdot(H_2O)_4\}_n$ is lesser than $\{[Zn(NH_2\text{-bdc})_2(4\text{-bpdb})]\cdot(H_2O)_4\}_n$ due to the presence of additional methyl groups in the pore channel. Both the dehydrated frameworks of $\{[Zn(NH_2\text{-bdc})_2(4\text{-bpdb})]\cdot(H_2O)_4\}_n$ and $\{[Zn_2(NH_2\text{-bdc})(4\text{-bpdh})]\cdot(H_2O)_4\}_n$ show a type-I selective CO_2 uptake profiles over N_2 up to 34.5 and 18.3 $cm^3\ g^{-1}$ at 195 K and 1 bar pressure (Figure: 3c, d), respectively. Different CO_2 uptake capacities of both the compounds have been corroborated to their respective void spaces, viz., 27.1 and 17.1% for $\{[Zn(NH_2\text{-bdc})_2(4\text{-bpdb})]\cdot(H_2O)_4\}_n$ and $\{[Zn_2(NH_2\text{-bdc})(4\text{-bpdh})]\cdot(H_2O)_4\}_n$, respectively.

2.1.2 Nitro Group-Decorated Pore Wall

Many groups[23, 25] anticipated that the nitro-functionalised MOFs always show less CO_2 uptake because of the bulky size of $–NO_2$ group, but our recent investigations[26, 27] interestingly show the elegant CO_2 selectivity over other non-polar gases like H_2, N_2, CH_4 as demonstrated by nitro-functionalised MOFs. Basically, the nitro group accumulates significant amount of negative charge on its oxygen atoms, which play an active role in binding with the quadrupolar CO_2 molecules. The single-crystal structure clearly indicates how a bulky group like nitro can show its desired functionality with its ideal orientation in the MOF. If the orientation of the nitro groups does not block the pore aperture, it can also act as an effective staff for designing MOFs with

selective CO_2 uptake. Thus, the crystal structure paved here into a new direction of thinking that the bulky groups will not be a factor for showing porous functionality if those are properly oriented in an MOF.

Two nitro-functionalised 3D Cu(II)-MOFs[26] were prepared with two different 4-pyridyl linkers, $\{[Cu(azbpy)(2\text{-ntp})]\cdot H_2O\}_n$ and $\{[Cu(4\text{-bpdb})(2\text{-ntp})]\cdot 2(H_2O)\}_n$ (2-ntp^{2-}=2-nitroterephthalate, azbpy=4,4′-azobispyridine and 4-bpdb=*N*,*N*′-bis-pyridin-4-ylmethylenehydrazine). In both the compounds, the ntp^{2-} bridges with the three Cu(II) centres form a 2D sheet, which are further pillared by the *N*,*N*′-donor linkers resulting in the formation of two different 3D structures (Figure: 4a, b). The channel dimensions and total solvent accessible void spaces are 6.5 × 3.0 $Å^2$ and 32.7% for $\{[Cu(azbpy)(2\text{-ntp})]\cdot H_2O\}_n$

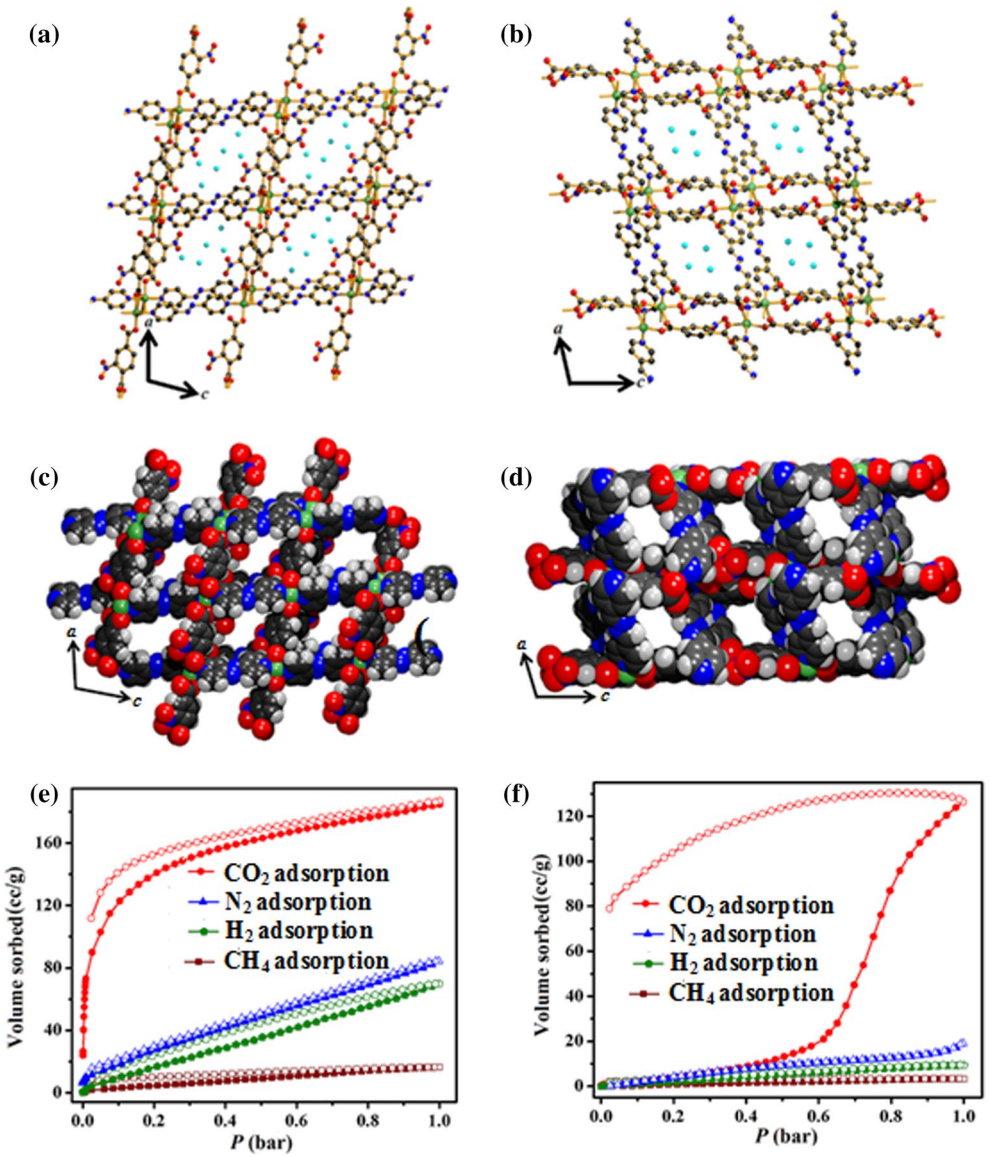

Figure 4: **a**, **b** 3D structure with water-filled 1D channels in $\{[Cu(azbpy)(2\text{-ntp})]\cdot H_2O\}_n$ and $\{[Cu(4\text{-bpdb})(2\text{-ntp})]\cdot 2(H_2O)\}_n$. **c**, **d** Space-filling models of dehydrated frameworks showing the 1D empty channels in $\{[Cu(azbpy)(2\text{-ntp})]\cdot H_2O\}_n$ and $\{[Cu(4\text{-bpdb})(2\text{-ntp})]\cdot 2(H_2O)\}_n$, respectively. **e**, **f** Selective CO_2 adsorption isotherms (at 195 K) over H_2 (at 77 K), N_2 (at 77 K) and CH_4 (at 298 K) gases for $\{[Cu(azbpy)(2\text{-ntp})]\cdot H_2O\}_n$ and $\{[Cu(4\text{-bpdb})(2\text{-ntp})]\cdot 2(H_2O)\}_n$, respectively. The *filled* and *open symbols* represent the adsorption and desorption isotherms, respectively. Reproduced with permission from Ref.[26] Copyright© 2016, American Chemical Society.

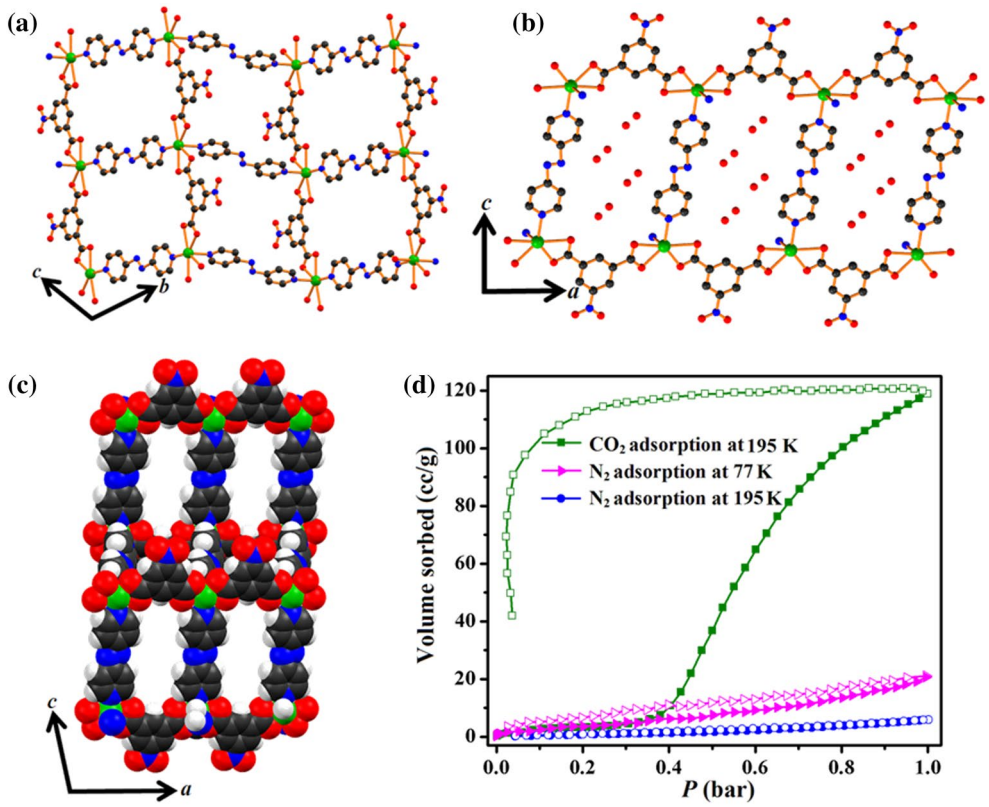

Figure 5: **a** A wavy 2D sheet constructed through both the azbpy and NO_2-bdc^{2-} ligands in $\{[Cd(azbpy)(NO_2\text{-}bdc)\cdot H_2O]\cdot 2H_2O\}_n$. **b** Guest water-filled 1D channels in $\{[Cd(azbpy)(NO_2\text{-}bdc)\cdot H_2O]\cdot 2H_2O\}_n$ along the *b*-axis. **c** Space-filling models of dehydrated framework showing 1D empty channel view along the *b*-axis. **d** Selective CO_2 adsorption isotherms (at 195 K) over N_2 (at 77 and 195 K); *filled* and *open symbols* represent adsorption and desorption isotherms, respectively. Reproduced with permission from Ref.[27] Copyright© 2016, American Chemical Society.

and 6.1 × 3.8 $Å^2$ and 28.5% for $\{[Cu(4\text{-}bpdb)(2\text{-}ntp)]\cdot 2(H_2O)\}_n$ (Figure: 4c, d), respectively, which are comparable also. But, interestingly, the projection of nitro groups is different, as the former cases are properly aligned with the pore and hence have greater CO_2 uptake than $\{[Cu(4\text{-}bpdb)(2\text{-}ntp)]\cdot 2(H_2O)\}_n$, where the nitro groups are not aligned towards the pore. However, both the dehydrated frameworks show appreciable selective CO_2 uptake over negligible uptake of H_2, N_2 and CH_4 gases (Figure: 4e, f) at ambient pressure due to the presence of properly oriented bulky, but polar nitro group, which does not have any effect on the voids of the MOFs.

Recently our group also reported selective CO_2 uptake in another nitro-functionalised 2D MOFs[27] $\{[Cd(azbpy)(NO_2\text{-}bdc)\cdot H_2O]\cdot 2H_2O\}_n$ [azbpy=4,4′-azobispyridine and NO_2-bdc^{2-}=5-nitro-1,3-benzenedicarboxylate], where the nitro group also faced towards the pore channel. Here, the dicarboxylate bridges with adjacent two Cd(II) centres through bis-chelating fashion to form a 1D chain which is further pillared by the azbpy linker resulting in the formation of a wavy 2D sheet (Figure: 5a). The 2D sheet also contains 1D water-filled channel along the *b*-axis (Figure: 5b). The channel dimension of 10.8 × 3.8 $Å^2$ (Figure: 5c) is pretty good for gas adsorption and the dehydrated framework exhibits type-V CO_2 uptake isotherms up to 119 cc/g at 195 K and 1 bar pressure, where N_2 uptake capacity is negligible (Figure: 5d). The pore channel in $\{[Cd(azbpy)(NO_2\text{-}bdc)\cdot H_2O]\cdot 2H_2O\}_n$, being nitro group centric and azo-functionalised, the quadrupolar CO_2 gas molecules are selectively adsorbed over the non-polar N_2 gas.

2.1.3 Azo-Azine Group-Decorated Pore Wall

Like other polar groups, the azo (–N=N–) and/or azine [–C(R)=N–N=C(R)–] groups in MOFs can also play an active role to show selective CO_2

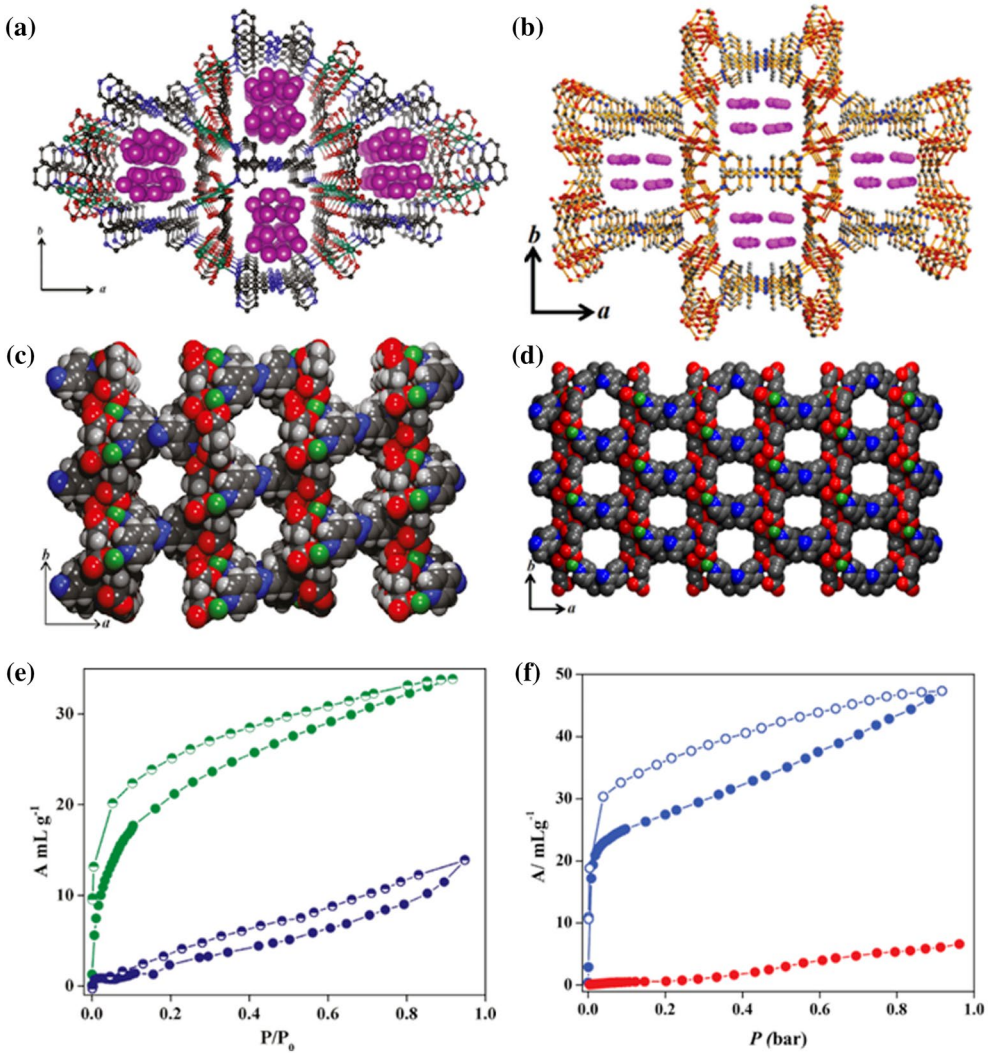

Figure 6: **a**, **b** Honeycomb-like 3D structures with guest water-filled 1D channel along *c*-axis for $\{[Cu(azpy)(glut)](H_2O)_2\}_n$ and $\{[Cu(Meazpy)_{0.5}(glut)](H_2O)\}_n$, respectively. **c**, **d** Space-filling model showing the empty pore channel along the *c*-axis for $\{[Cu(azpy)(glut)](H_2O)_2\}_n$ and $\{[Cu(Meazpy)_{0.5}(glut)](H_2O)\}_n$, respectively. **e** Selective CO_2 sorption isotherms over N_2 for $\{[Cu(azpy)(glut)](H_2O)_2\}_n$; CO_2 (*green*) at 195 K and N_2 (*blue*) at 77 K. **f** Selective CO_2 sorption isotherms over N_2 for $\{[Cu(Meazpy)_{0.5}(glut)](H_2O)\}_n$; CO_2 (*blue*) at 195 K and N_2 (*red*) at 77 K; filled and empty symbols signifying the adsorption and desorption isotherms, respectively. Reproduced with permission from Ref. [28]. Copyright© 2011, American Chemical Society for $\{[Cu(azpy)(glut)](H_2O)_2\}_n$ and from Ref.[29] Copyright© 2014, Royal Society of Chemistry for $\{[Cu(Meazpy)_{0.5}(glut)](H_2O)\}_n$.

adsorption over other non-polar gases. When the pore walls of MOFs are decorated with azo and/or azine groups, then the CO_2 molecules bind easily with their Lewis acidic carbon centre due to the quadrupole moment of the CO_2 molecule. Here, we discuss the effect of this group with three examples from our work.[28–30]

We synthesised two azine group-functionalised 3D Cu(II)-MOFs,[28, 29] namely, $\{[Cu(azpy)(glut)](H_2O)_2\}_n$ and $\{[Cu(Meazpy)_{0.5}(glut)](H_2O)\}_n$ [where, azpy=*N*,*N*′-bis-pyridin-4-ylmethylene-hydrazine and Meazpy=*N*,*N*′-bis-(1-pyridin-4-ylethylidene)hydrazine] with a combination of glutarate (glut) and two differently substituted azine linkers. Both the compounds form a paddle-wheel $Cu_2(CO_2)_4$ units which are connected by both the glutarate and *N*,*N*′-donor linkers in a crisscross fashion; resulting in the formation of honeycomb-like 3D structures with guest water-filled 1D channel (Figure: 6a, b). The pore surfaces of both the structures contain azine groups and the effective solvent accessible voids

are 34 and 28% for $\{[Cu(azpy)(glut)](H_2O)_2\}_n$ and $\{[Cu(Meazpy)_{0.5}(glut)](H_2O)\}_n$ (Figure: 6c, d), respectively, showing selective CO_2 uptake over N_2 (Figure: 6e, f). In quite a general way, $\{[Cu(azpy)(glut)](H_2O)_2\}_n$ has greater pore volume than $\{[Cu(Meazpy)_{0.5}(glut)](H_2O)\}_n$ due to the absence of additional methyl group in the azpy linker, but interestingly $\{[Cu(Meazpy)_{0.5}(glut)](H_2O)\}_n$ exhibits 50% greater CO_2 uptake (~9 wt%) than $\{[Cu(azpy)(glut)](H_2O)_2\}_n$ (~6 wt%) (Figure: 6e, f). This is due to the +I effect of the $-CH_3$ group in Meazpy, which increases the Lewis basicity of the –C=N– group aligned in the pore wall of dehydrated $\{[Cu(Meazpy)_{0.5}(glut)](H_2O)\}_n$.

Our group also reported two other azo/azine group-functionalised 3D MOFs[30] of Cd(II) metal ions with the combination of succinate dianion (suc) and two different 4-pyridyl linkers. Both the compounds $\{[Cd(L1)(suc)]\cdot(H_2O)_3\}_n$ and $\{[Cd(L2)(suc)]\cdot(H_2O)_2\}_n$ [where, L1 = 2,5-Bis-(4-pyridyl)-3,4-diaza-2,4-hexadiene, L2 = trans 4,4′-azobispyridine] show honeycomb-like 3D structures containing guest water-filled 1D

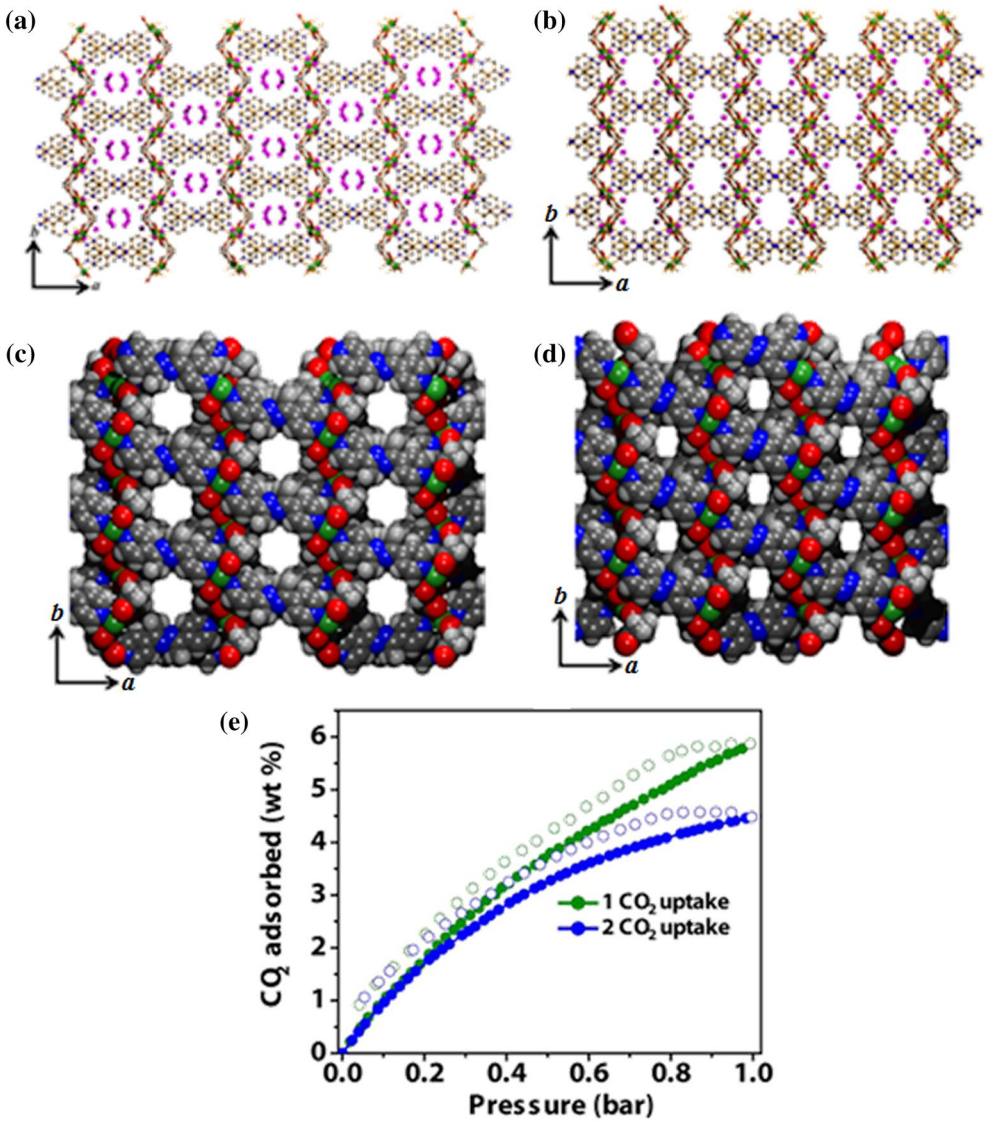

Figure 7: **a**, **b** Honeycomb-like 3D structure with guest water-filled 1D channels in $\{[Cd(L1)(suc)]\cdot(H_2O)_3\}_n$, $\{[Cd(L2)(suc)]\cdot(H_2O)_2\}_n$. **c**, **d** *Space-filling* models showing empty 1D channels in dehydrated frameworks of $\{[Cd(L1)(suc)]\cdot(H_2O)_3\}_n$ and $\{[Cd(L2)(suc)]\cdot(H_2O)_2\}_n$. **e** CO_2 adsorption isotherms for $[Cd(L1)(suc)]_n$ (*green*) and $[Cd(L2)(suc)]_n$ (*blue*) at 273 K temperature and 1 atm. pressure; *filled* and *open circles* signify the adsorption and desorption, respectively. Reproduced with permission from Ref.[30] Copyright© 2012, American Chemical Society.

channels along the *c*-axis (Figure: 7a, b). The channel dimensions of the dehydrated frameworks of $\{[Cd(L1)(suc)]\cdot(H_2O)_3\}_n$ and $\{[Cd(L2)(suc)]\cdot(H_2O)_2\}_n$ are 4.4 × 5.3 Å^2 and 4.2 × 3.1 Å^2 (Figure: 7c, d), respectively. The dehydrated frameworks of $\{[Cd(L1)(suc)]\cdot(H_2O)_3\}_n$ and $\{[Cd(L2)(suc)]\cdot(H_2O)_2\}_n$ show selective CO_2 uptake up to 5.86 and 4.47 wt% at 273 K and ~1 atm pressure; in a reversible way, respectively (Figure: 7e).

2.2 Tuning of Pore Sizes and Dimensions

Like the modulation of pore wall functionality, the control of pore size and dimension is also a crucial factor in the design of MOFs showing enhanced selective CO_2 uptake. When the pore aperture of MOFs is commensurate with adsorbed gas molecules, then MOFs exhibit porosity to such adsorbed gas molecules. The kinetic diameter of CO_2 and N_2 is closely comparable, so it will be very difficult for selective CO_2 adsorption over N_2 through the tuning of pore size of MOFs. However, a critical investigation of crystal structure will illuminate on issues related to pore size of synthesised MOFs. Several reports[31, 32] exist on controllable pore sizes along with modified pore environment through judicious tuning of length as well as introduction of polar functional groups in the structure of templates used. The kinetic diameter of N_2 molecule is comparatively larger than that of CO_2 molecule and has no polarity for N_2; it is difficult to enter the voids due to the blocking of one-dimensional (1D) channels. However, CO_2 molecule has quadrupole moment and smaller kinetic diameter (3.3 Å); hence, it can be adsorbed over N_2 (3.64 Å) only selectively. Here, we discuss some representative examples of controlling pore sizes of MOFs to learn of their selective CO_2 uptake capacity.

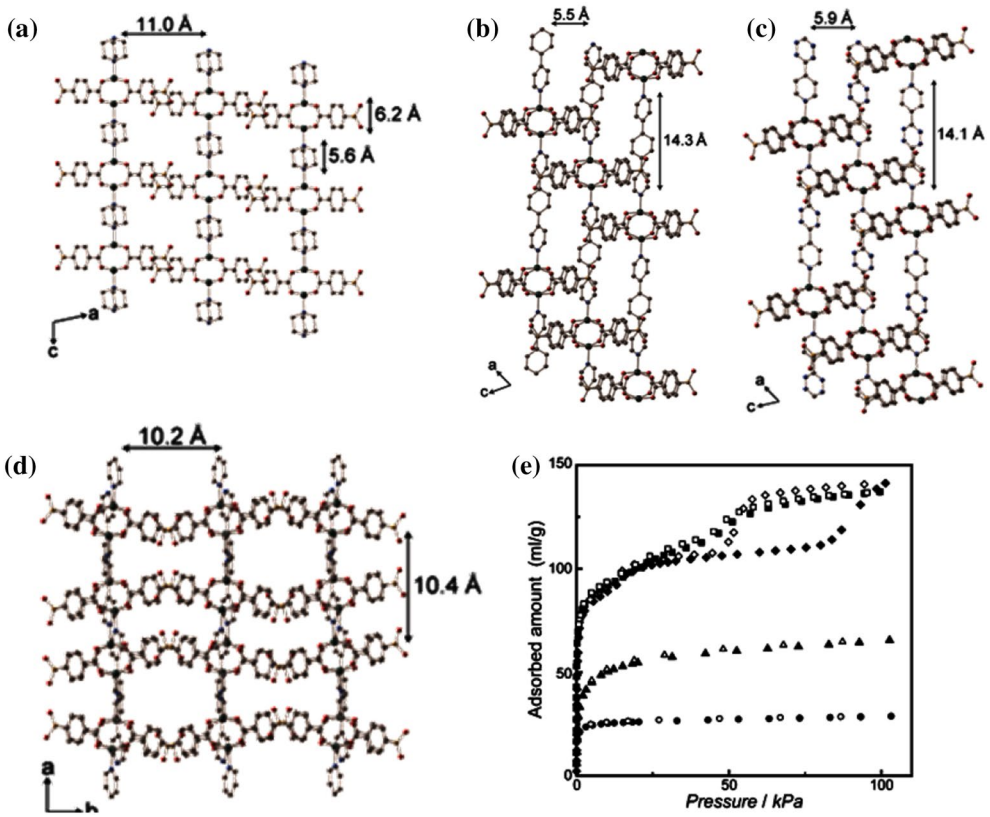

Figure 8: **a**–**d** Structural component of compounds $[Zn_2(sdb)_2(dabco)]_n$, $[Zn_2(sdb)_2(bpb)]_n$, $[Zn_2(sdb)_2(bpt)]_n$ and $[Zn_2(sdb)_2(bpy)]_n$, respectively, showing the dimensions of pore channels; the solvent molecules are omitted for clarity. **e** CO_2 sorption isotherms at 195 K, where *triangle-*, *square-*, *diamond-* and *circle-shaped symbols* represent sorption isotherms for the compounds. *Open* and *filled symbols* signify the adsorption and desorption isotherms, respectively. Reproduced with permission from Ref.[31] Copyright© 2013, American Chemical Society.

In this context, Kitagawa et al.[31] reported the synthesis of four different types of 4,4′-sulfonyldibenzoate (sdb)-based Zn(II) MOFs, namely, $[Zn_2(sdb)_2(dabco)]_n$, $[Zn_2(sdb)_2(bpb)]_n$, $[Zn_2(sdb)_2(bpt)]_n$ and $[Zn_2(sdb)_2(bpy)]_n$ by varying the *N*,*N*′-donor linkers, 1,4-diazabicyclo[2,2,2]octane (dabco), 1,4-bis(4-pyridyl) benzene (bpb), 3,6-bis(4-pyridyl)-1,2,4,5-tetrazine (bpt), and 4,4′-bipyridyl (bpy) Due to the different length and structural motif of *N*,*N*′-donor linkers, the above compounds form versatile structures including interpenetrated/interdigitated and non-interpenetrated frameworks along with varying pore sizes and dimensions (Figure: 8a–d), which are reflected on the gas uptake capacity of the MOFs. The cross-sectional diameter of $[Zn_2(sdb)_2(dabco)]_n$ is 6.6 Å along the dabco ligands, where for $[Zn_2(sdb)_2(bpb)]_n$ and $Zn_2(sdb)_2(bpt)]_n$ are 6.6 Å along their respective *N*,*N*′-donor linkers. But for $[Zn_2(sdb)_2(bpy)]_n$, the diameter of the 1D channel is 3.3 Å along the *c*-axis. The CO_2 uptake in all the cases starts at very low pressure region and reaches as much as 66, 137, 141 and 29 mL g^{-1} for $[Zn_2(sdb)_2(dabco)]_n$, $[Zn_2(sdb)_2(bpb)]_n$, $[Zn_2(sdb)_2(bpt)]_n$ and $[Zn_2(sdb)_2(bpy)]_n$, respectively, at 195 K and $P/P_0 \approx 1.0$ (Figure: 8e). So it is an elegant example of the strategy to control pore size for selective adsorption of MOFs.

Our group reported recently three 3,4-pyridinedicarboxylate (3,4-pyrdc)-based MOFs,[32] namely, $\{[Cd_2(3,4\text{-pyrdc})_2(4,4\text{-bipy})(H_2O)_2]\cdot 4H_2O\}_n$, $\{[Mn_2(3,4\text{-pyrdc})_2(bpee)(H_2O)_2]\cdot H_2O\}_n$ and $\{[Cu_2(3,4\text{-pyrdc})_2(bpp)_2(H_2O)_4]\cdot 5H_2O\}_n$ [where, 4,4-bipy=4,4-bipyridine, bpee=1,2-bis(4-pyridyl)-ethylene and bpp=1,3-bis(4-pyridyl)-propane] by varying the metal ions along with *N*,*N*′-donor linkers. The compounds show different pore sizes and dimensions, which play an active role on gas uptake capacity to different extents. Compound $\{[Cd_2(3,4\text{-pyrdc})_2(4,4\text{-bipy})(H_2O)_2]\cdot 4H_2O\}_n$ exhibits a 3D framework with hexagonal and rectangular channels of dimensions 5.3 × 3.5Å and 4.7 × 2.0Å, respectively (Figure: 9a). Compound $\{[Mn_2(3,4\text{-pyrdc})_2(bpee)(H_2O)_2]\cdot H_2O\}_n$ shows a pillared-layer frameworks with guest water-filled channel along the *b*-axis (Figure: 9b), which basically does not show any significant pore channel. The compound $\{[Cu_2(3,4\text{- pyrdc})_2(bpp)_2(H_2O)_4]\cdot 5H_2O\}_n$ shows a supramolecular 3D structure with guest water-filled channel along the *c*-axis (Figure: 9c), where the dimension of the channel is 6.8 × 2.6Å. The N_2 adsorption amount of all the compounds is negligible. The CO_2 uptake capacity of the dehydrated frameworks of Cd(II), Mn(II) and Cu(II) are 39 cm^3 g^{-1} (7.7 wt%), 19 cm^3 g^{-1} (3.7 wt%), and 47 cm^3 g^{-1} (9.2 wt%) at 195 K, respectively (Figure: 9d), which are commensurate with their pore sizes. The CO_2/N_2 selectivities for Cd(II), Mn(II) and Cu(II) were 8.8, 3.7 and 9.3, respectively.

The interpenetration of MOFs[33] will also play a vital role on the pore aperture with diminishing void spaces. Generally, when a single network accommodates large voids, with two or more such networks mutually interpenetrated, it will result in the formation of interpenetrated MOFs with comparatively lower void spaces. So, in a quite general way, the interpenetrated MOFs containing small pores generated through interpenetration will exhibit lower CO_2 uptake capacity in most cases. On the contrary, interpenetrated structures in some cases will exhibit structural dynamicity[34, 35] showing gated adsorption properties,[10, 36] which is known as the "breathing" effect.[10, 36] In such cases, adsorption may increase even for an interpenetrated structure due to structural dynamicity.[34–36]

Recently, MOFs with different pore sizes and dimensions were also widely investigated for Xe/Kr adsorption selectivity similar to selective uptake of CO_2. The effect of pore sizes on Xe/Kr selectivity has been discussed by some groups,[37–40] which suggest that the MOFs with smaller pores (pore diameter just greater than the kinetic diameter of Xe molecule) exhibit high Xe/Kr selectivity than those with comparatively larger pores. This is because the small pores provide strong adsorption sites, mainly for Xe, which adsorbs more strongly than Kr due to van der Waals interactions and higher polarisability.

3 Electrical Conductance of MOFs

Like CO_2 storage and separation, conductivity is also an appealing functionality of MOFs independently as well as when coupled with other functionalities of MOFs to prepare smart materials. Thus, it has an immense potential for opening up the door of a new El Dorado of tailor-made Schottky barrier diodes, solar cells, light-emitting diodes and suitable memory devices.[41] Though a good number of conventional covalent polymers were potentially used to measure electrical conduction in the field of material science, the search for this property in MOFs is very limited mostly due to the lack of understanding of structure–property relationship for this particular property. The gradual incorporation of theoretical calculations in MOFs seems to be a powerful tool for experimental measurements and for rational design of new conductive MOFs as well as for nascent electronic device fabrication. Realising

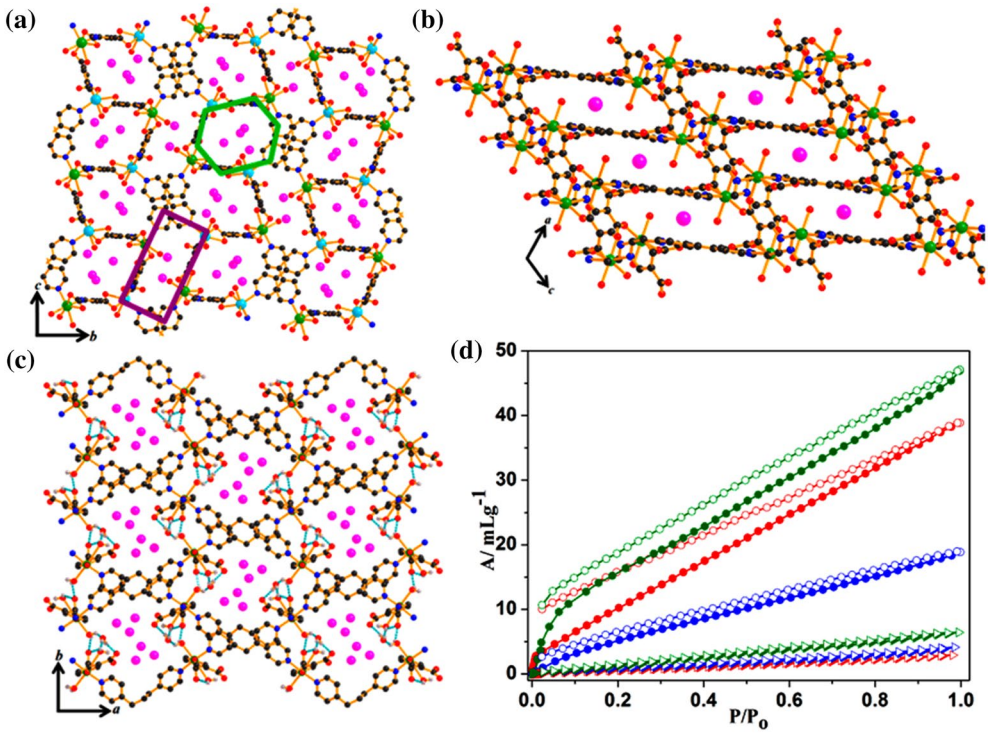

Figure ***9:*** A view of the **a** 3D network with guest water-filled *hexagonal-* and *rectangular-shaped* channels along the *a*-axis in $\{[Cd_2(3,4\text{-pyrdc})_2(4,4\text{-bipy})(H_2O)_2]\cdot 4H_2O\}_n$, and **b** 3D pillared-layer frameworks with guest water-filled channel in $\{[Mn_2(3,4\text{-pyrdc})_2(bpee)(H_2O)_2]\cdot H_2O\}_n$. **c** Supramolecular 3D structure with guest water-filled channel in $\{[Cu_2(3,4\text{-pyrdc})_2(bpp)_2(H_2O)_4]\cdot 5H_2O\}_n$. **d** CO_2 (*circles*) and N_2 (*triangles*) adsorption isotherms (*solid symbols*) and desorption isotherms (*open symbols*) of dehydrated framework for $\{[Cd_2(3,4\text{-pyrdc})_2(4,4\text{-bipy})(H_2O)_2]\cdot 4H_2O\}_n$ (*red*), $\{[Mn_2(3,4\text{-pyrdc})_2(bpee)(H_2O)_2]\cdot H_2O\}_n$ (*blue*) and $\{[Cu_2(3,4\text{-pyrdc})_2(bpp)_2(H_2O)_4]\cdot 5H_2O\}_n$ (*green*) measured at 195 K for CO_2 and 77 K for N_2. Reproduced with permission from Ref.[32] Copyright© 2016, American Chemical Society.

the importance of such study for the fabrication of versatile electronic devices, contemporary synthetic researchers have recently focussed their attention on designing MOF-based materials with high electrical conductivity. There are reports[13] of low- (i.e. 1D) or higher-dimensional (i.e. 2D/3D) CPs for electrical conductivity measurement, but the structure–property relationship has not been well understood. As mentioned, we have extracted the knowledge from single-crystal X-ray structure and tried to correlate the electrical conductivity of MOFs with their structures. The organic ligands placed in the pore of the MOFs show high electrical conductivity[42, 43] of a non-charged MOF, a supposed insulator.

Our group[36] has reported a 2D Cd(II)-MOF, $\{[Cd_2(azbpy)_2(HO\text{-}1,3\text{-}bdc)_2](azbpy).(H_2O)\}_n$,[42] (where OH-1,3-bdc=5-hydroxy-1,3-benzenedicarboxylate and azbpy=4,4′-azobispyridine), where the dicarboxylate bridges Cd(II) centres to form an infinite 1D ladder that is pillared by the azbpy ligand resulting in the formation of a 2D sheet (Figure: 10a). The 2D sheet is extended to a supramoleculer 3D structure through intermolecular π–π interactions with the free azbpy ligand (Figure: 10b). This structure of the MOF with organic ligands in the pore prompted us to measure its electrical conductivity. The thin film made with the microcrystalline samples of Cd(II)-MOF exhibits electric conductivity up to 1.86 S cm^{-1} (Figure: 10c) at room temperature and pressure, and the current–voltage curve indicates *n*-type semiconducting behaviour. Prior to this report, no other 2D or 3D MOFs containing free organic ligands has been reported in the literature showing such remarkable electrical conductivity in crystalline form.

The appreciable value of conductivity has also encouraged us to fabricate an electronic device to see its performance as a semiconducting material. The band gap measured experimentally was 2.0 eV, which is closely identical to its theoretical value (2.07 eV). The calculated position of Fermi level and the population in the block orbital also

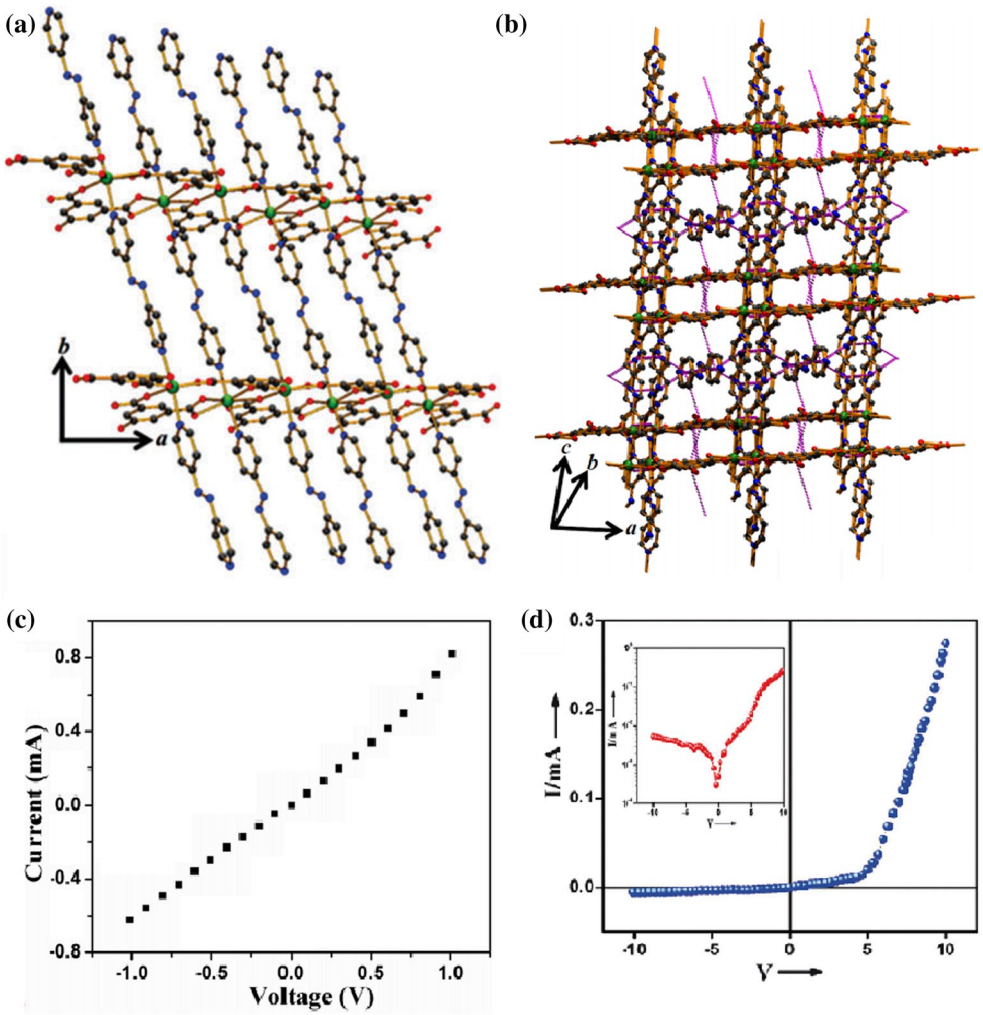

Figure 10: **a** The 2D sheet containing a 1D ladder with the azbpy linker. **b** Supramolecular 3D structure (π–π interactions *pink dotted lines*) in $\{[Cd_2(azbpy)_2(HO\text{-}1,3\text{-}bdc)_2](azbpy).(H_2O)\}_n$. **c** Current–voltage plot for conductivity measurement of $\{[Cd_2(azbpy)_2(HO\text{-}1,3\text{-}bdc)_2](azbpy)\cdot(H_2O)\}_n$. **d** Current (*I*)–voltage (*V*) characteristics of the ITO/Cd-MOF/Al device on linear and logarithmic (*inset* of the figure) scales. Reproduced with permission from Ref.[42] Copyright© 2014, Royal Society of Chemistry.

prove its *n*-type semiconducting nature. However, the values of its electrical conductivity and band gap have encouraged us to make a Schottky barrier diode by fabricating the sandwiched configuration of indium tin oxide (ITO)/Cd-MOF/aluminium (Al), where Al electrode was used as a background for rectifying Schottky barrier diode for its high work function value (4.08 eV). The fabricated Al/Cd-MOF/ITO-based device exhibits a nonlinear behaviour with an on/off current ratio in the order of $\sim 10^2$ (at ± 10 V) signifying rectification (Figure: 10d). Our work is the first example of an MOF-based electronic device as a Schottky barrier diode, which has its inspiration from an understanding of single-crystal X-ray structure.

In continuation of our previous work, recently our group also reported two Zn(II)-MOFs,[43] $\{[Zn(azbpy)(HO\text{-}1,3\text{-}bdc)(H_2O)]\cdot(azbpy)\}_n$ and $\{[Zn(azbpy)_{0.5}(HO\text{-}1,3\text{-}bdc)\ (C_2H_5OH)]\cdot(H_2O)\}_n$ using the same 5-hydroxyisophthalate (HO-1,3-bdc) and 4,4′-azobispyridine (azbpy) ligands. Compound $\{[Zn(azbpy)(HO\text{-}1,3\text{-}bdc)(H_2O)]\cdot(azbpy)\}_n$ exhibits a 2D sheet by bridging both *N*,*N*′-donor azbpy ligand and chelating-monodentate HO-1,3-bdc^{2-} with the Zn^{2+} centres. This was extended to a supramolecular 3D structure through intermolecular H-bonding

and π–π interactions with free azbpy ligands (Figure: 11a). But, for compound $\{[Zn(azbpy)_{0.5}(HO\text{-}1,3\text{-}bdc)(C_2H_5OH)]\cdot(H_2O)\}_n$, the dicarboxylate bridges with Zn(II) centres in a bidentate bridging fashion to form a 1D ladder, which was further pillared by azbpy ligand to form a 2D structure (Figure: 11b). Both the MOFs have almost similar structure, but the first one contains lattice azbpy ligands in its void spaces, whereas the second one contains water molecules. Both the MOFs show electrical conductivity up to 1.1×10^{-4} and 2.5×10^{-5} S cm^{-1} (Figure: 11c), respectively, at room temperature which means that the MOF with lattice azbpy ligands in its void exhibits nearly ten times greater conductivity than water-containing $\{[Zn(azbpy)_{0.5}(HO\text{-}1,3\text{-}bdc)(C_2H_5OH)]\cdot(H_2O)\}_n$. Being volatile, water will not be present in the void at the thin film preparation temperature and hence it is clear that the free azbpy ligand into the void spaces; definitely delivers an extra path for charge transfer. The direct band gaps of the compounds conform to theoretical calculations suggesting *p*-type semiconductivity in both. The presence of additional free organic ligand in the voids of $\{[Zn(azbpy)(HO\text{-}1,3\text{-}bdc)(H_2O)]\cdot(azbpy)\}_n$ has also generated a higher electronic level near the Fermi level. This example of two-model conductor MOFs helps our understanding for creating good conducting MOFs by lattice organic ligand in the pore. Like the previous case, we have also studied the rectification behaviour of the device, prepared in the same manner (ITO/MOF/Al) as of these two compounds. The on/off current ratios are 4.9 and 3.2 at ±1 V (Figure: 11d) and the potential barriers of the fabricated devices are 0.27 and 0.43 eV for $\{[Zn(azbpy)(HO\text{-}1,3\text{-}bdc)(H_2O)]\cdot(azbpy)\}_n$ and $\{[Zn(azbpy)_{0.5}(HO\text{-}1,3\text{-}bdc)(C_2H_5OH)]\cdot(H_2O)\}_n$, respectively. As discussed, these values also support better electronic behaviour in MOFs where ligands are present in the pores of frameworks.

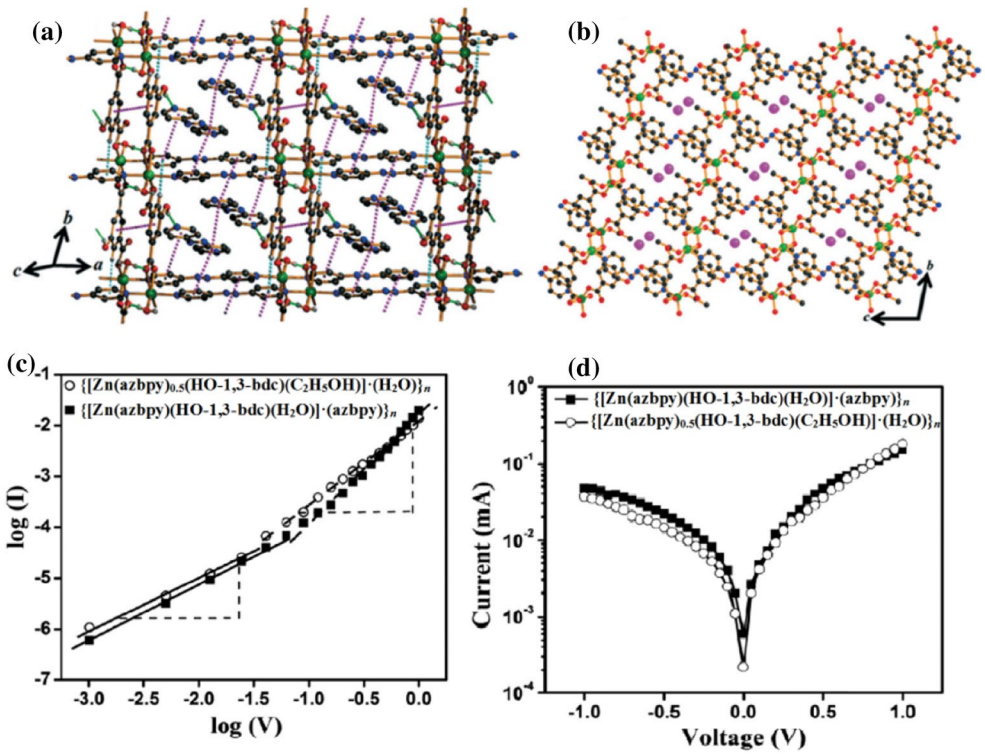

Figure 11: **a** Supramolecular 3D structure in $\{[Zn(azbpy)(HO\text{-}1,3\text{-}bdc)(H_2O)]\cdot(azbpy)\}_n$ through locking of the 2D sheets and free azbpy ligands by intermolecular H-bonding and π–π interactions. **b** 2D sheet in $\{[Zn(azbpy)_{0.5}(HO\text{-}1,3\text{-}bdc)(C_2H_5OH)]\cdot(H_2O)\}_n$ constructed by HO-1,3-bdc and azbpy ligand. **c** Logarithmic current–voltage plot for conductivity measurement, and **d** current–voltage plots of the fabricated sandwich devices for both the compounds. Reproduced with permission from Ref.[43] Copyright© 2016, Royal Society of Chemistry.

4 Structure of CPs Guiding Chemical (Redox) Transformation

The most striking exploration by our group in the field of CPs is framework-supported reduction. Interestingly, the phenomenon was observed in an in situ chemical process and the observation of a crystal structure inspired us into this investigation. This is a fine example of the X-ray structure, paving the way for understanding the redox chemistry from a newer dimension. We have isolated three different coordination polymers (CPs),[44] namely, $\{[Cd(3\text{-}bpdb)(Cl)]\cdot ClO_4\}_n$,$\{[Cd(3\text{-}bpdb)_3(H_2O)_2]\cdot(3\text{-}bpdb)(ClO_4)_2\}_n$ and $\{[Cd(3\text{-}bpdb)(suc)(H_2O)_2]\cdot(H_2O)_2\}_n$ with the combination of cadmium perchlorate, 1,4-bis(3-pyridyl)-2,3-diaza-1,3-butadiene (3-bpdb) and disodium succinate (Na_2suc) from the same reaction. The first one among the three, i.e. $\{[Cd(3\text{-}bpdb)(Cl)]\cdot ClO_4\}_n$ shows an α-polonium-type 3D coordination network created by an exactly perpendicular Cl–Cd–Cl linkage, and also contains ClO_4^- ion-filled 1D channel (Figure: 12a, b). We have neither used any cadmium chloride salt nor have we added any other chloride salt externally to the reaction mixture. Besides, there is no provision for chloride to come from the solvent or any other impurity, as all the reactions are performed in chloride-free water. Thus, after ruling over the human error and unknown impurity factor, this Cl^--integrated 3D framework of $\{[Cd(3\text{-}bpdb)(Cl)]\cdot ClO_4\}_n$ really became an interesting research problem for us. Therefore, we started enthusiastically to find the source of Cl^- ion, as we were confident then that it originated from some in situ chemical route. Finally, we realised that the chloride had been produced from the reduction of perchlorate used in the reaction. To account for the presence of electrons in reduction, we searched the parallel oxidation process and came across a very interesting finding. We performed a GC–MS experiment with the reaction mixture and observed the formation of nicotinamide produced by the oxidation of 3-bpdb (Figure: 12c). Similarly, the ESI-MS data of the reaction mixture confirms the formation of nicotinamide at *m*/*z* 122.04 (Figure: 12d) and IR spectral data [ν(C=O), 1636 cm^{-1} (stretch), ν(N–H), 3444 cm^{-1} (stretch) and 1549 cm^{-1} (bending)] also confirm it as the product of the

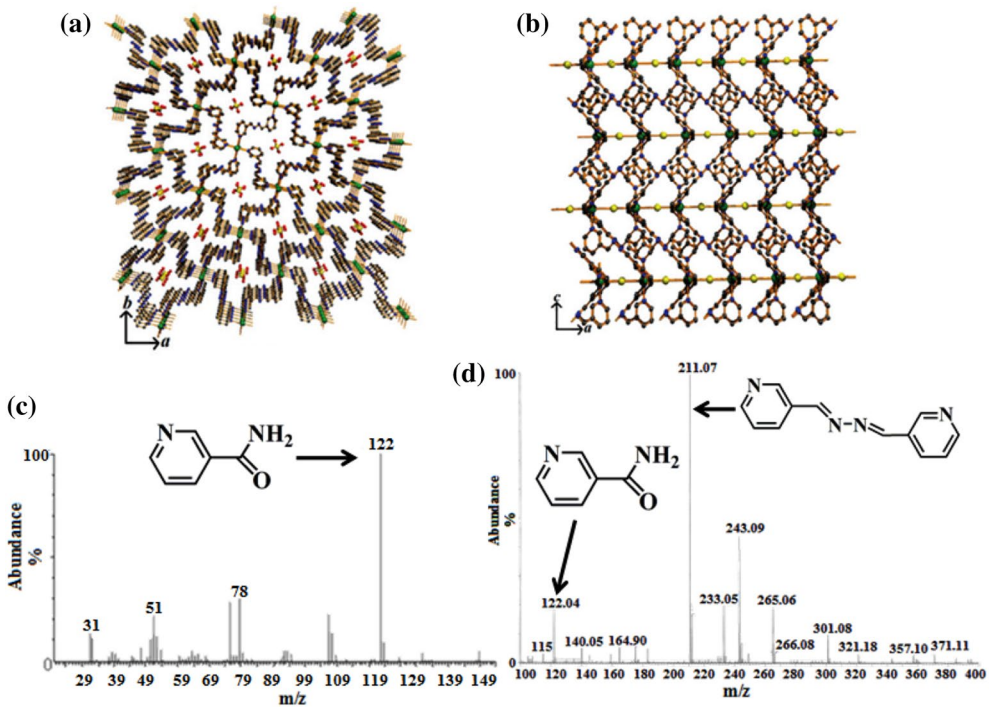

Figure 12: **a** 3D framework of $\{[Cd(3\text{-}bpdb)(Cl)]\cdot ClO_4\}_n$ showing the channels occupied by the ClO_4^- anions. **b** 3D framework in $\{[Cd(3\text{-}bpdb)(Cl)]\cdot ClO_4\}_n$ showing the Cl–Cd–Cl rod in the crystallographic *c*-axis. **c** Mass spectra of the peak at 10.37 min from the GC trace of the resulting amide from the oxidation of imine in the reaction medium. **d** ESI mass spectrum of the resulting *yellow* residue. Reproduced with permission from Ref.[44] Copyright© 2013, Royal Society of Chemistry.

oxidation of imine along with parallel reduction of perchlorate to chloride. To confirm the transformation of perchlorate to chloride, we also performed reactions under the same conditions, but by varying the reactants as well as their ratios (Table: 1). Considering the emergence of nicotinamide as a signature for formation of chloride, we conclude that the evolution of $\{[Cd(3\text{-bpdb})(Cl)]\cdot ClO_4\}_n$ from the reduction of perchlorate is independent of the nature of perchlorate anion or the presence of other counter anions. The framework structure has an important role in the transformation.

The logic of this interesting observation justifies the continuation of our interest in this work, where we have modified the non-substituted 3-bpdb linker into methyl-substituted 2,5-bis-(3-pyridyl)-3,4-diaza-2,4-hexadiene (3-bpdh). We have synthesised two different Cd(II)-CPs,[45] namely, $[Cd(3\text{-bpdh})_2(ClO_4)_2]_n$ and $\{[Cd(3\text{-bpdh})(suc)(H_2O)]\cdot 3(H_2O)\}_n$ using *N*,*N*′-donor 3-bpdh and disodium succinate (suc). Compound $[Cd(3\text{-bpdh})_2(ClO_4)_2]_n$ exhibits a 1D chain containing coordinated perchlorate anions (Figure: 13a). It is important to note here that we have obtained the perchlorate coordinated product instead of chloride. The absence of chloride is supported by the absence of any oxidation or reduction process in the GC–MS/ESI-MS study (Figure: 13b, c). The presence of methyl substituent on 3-bpdh linker gives it a stable C–C bond instead of the labile C–H bond in 3-bpdb and hints that to get any chloride-containing product through reduction, the N-donor ligand used must be oxidised simultaneously.

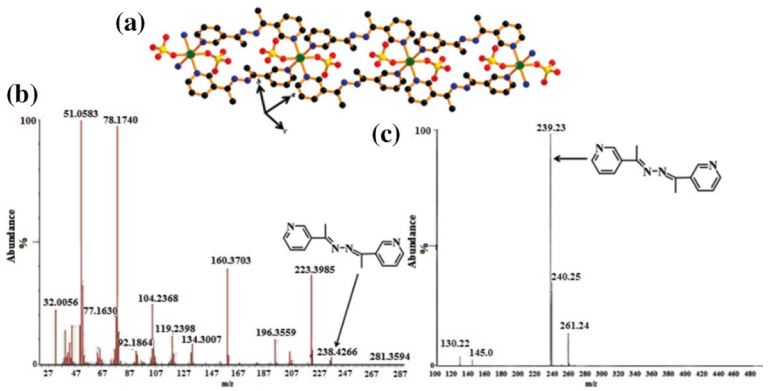

Figure 13: **a** 1D chain structure constructed through 3-bpdh ligand and coordinated perchlorate ions in $[Cd(3\text{-bpdh})_2(ClO_4)_2]_n$. **b** Appearance of a mass of 3-bpdh ligand (i.e. 238.4266) in the reaction mixture observed by GC–MS study. **c** ESI mass spectrum of *yellow* residue in the reaction mixture. Reproduced with permission from Ref.[45] Copyright© 2015, Royal Society of Chemistry.

Table 1: Formation of amide with different reactants and varying ratios.

No.	Reaction	Reactant ratio	Formation of amide
I	3-bpdb + $Cd(ClO_4)_2\cdot 6H_2O$	1:1	Yes
II	3-bpdb + $Cd(ClO_4)_2\cdot 6H_2O$ + Na_2suc	1:1:1	Yes
III	3-bpdb + $Cd(NO_3)_2\cdot 4H_2O$ + $NaClO_4$	1: 1: 2	Yes
IV	3-bpdb + $Cd(ClO_4)_2\cdot 6H_2O$	2:1	No
V	3-bpdb + $Cd(ClO_4)_2\cdot 6H_2O$	3:1	No
VI	3-bpdb + $Cd(ClO_4)_2\cdot 6H_2O$	4:1	No
VII	3-bpdb + $NaClO_4$	1: 2	No

5 Conclusion

The potential application of CPs and/or MOFs in different fields provides a concrete structure–property relationship which opens a window to understand the strategic design of functional CPs/MOFs. The outcome of X-ray structure has profound impact on structural parameters like pore sizes, pore environment, voids and lattice entities, the base parameters for the creation of structural database in functional CPs/MOFs. Here, we have tried not only to correlate the versatile functionality of mixed-ligand CPs/MOFs, but also investigated an interesting chemical transformation through X-ray crystallography. For research involving the design of CPs/MOFs, X-ray crystallography stands out as an important characterisation tool, as it sometimes opens up a new horizon in research in chemical and material science.

Acknowledgements

We acknowledge the financial assistance of SERB, India (Grant No. SB/S1/IC-06/2014). D.K.M. acknowledges UGC for his research fellowship.

Received: 18 January 2017 Accepted: 10 February 2017
Published online: 3 July 2017

References

1. Desiraju GR (2014) Some themes in chemical crystallography pertinent to the Indian contribution. J Indian Inst Sci 94:1–8
2. Desiraju GR (1989) Crystal engineering: the design of organic solids. Elsevier, Amsterdam
3. Moulton B, Zaworotko MJ (2001) From molecules to crystal engineering: supramolecular isomerism and polymorphism in network solids. Chem Rev 101:1629–1658
4. He Y, Li B, O'Keeffec M, Chen B (2014) Multifunctional metal–organic frameworks constructed from meta-benzenedicarboxylate units. Chem Soc Rev 43:5618–5656
5. Zhang Z, Zhao Y, Gong Q, Lib Z, Li J (2013) MOFs for CO_2 capture and separation from flue gas mixtures: the effect of multifunctional sites on their adsorption capacity and selectivity. Chem Commun 49:653–661
6. Zhao D, Timmons DJ, Yuan D, Zhou H-C (2011) Tuning the topology and functionality of metal–organic frameworks by ligand design. Acc Chem Res 44:123–133
7. Chakraborty A, Maji TK (2014) Structural diversities in metal-organic coordination polymers based on flexibility in organic spacer. J Indian Inst Sci 94:69–78
8. Li J-R, Sculley J, Zhou H-C (2012) Metal-organic frameworks for separations. Chem Rev 112:869–932
9. Bhattacharya B, Ghoshal D (2015) Selective carbon dioxide adsorption by mixed ligand porous coordination polymers. CrystEngComm 17:8388–8413
10. Nijem N, Wu H, Canepa P, Marti A, Balkus KJ Jr, Thonhauser T, Li J, Chabal YJ (2012) Tuning the gate opening pressure of metal–organic frameworks (MOFs) for the selective Separation of hydrocarbons. J Am Chem Soc 134:15201–15204
11. Dietzel PDC, Besikiotis V, Blom R (2009) Application of metal–organic frameworks with coordinatively unsaturated metal sites in storage and separation of methane and carbon dioxide. J Mater Chem 19:7362–7370
12. Lee JY, Farha OK, Roberts J, Scheidt KA, Nguyen ST, Hupp JT (2009) Metal–organic framework materials as catalysts. Chem Soc Rev 38:1450–1459
13. Givaja G, Amo-Ochoa P (2012) C.J. Go´mez-Garcı´a and F. Zamora, Electrical conductive coordination polymers. Chem Soc Rev 41:115–147
14. Kreno LE, Leong K, Farha OK, Allendorf M, Duyne RPV, Hupp JT (2012) Metal-organic framework materials as chemical sensors. Chem Rev 112:1105–1125
15. Bhattacharya B, Halder A, Paul L, Chakrabarti S, Ghoshal D (2016) Eye-catching dual-fluorescent dynamic metal–organic framework senses traces of water: experimental findings and theoretical correlation. Chem Eur J 22:14998–15005
16. Banerjee R, Phan A, Wang B, Knobler C, Furukawa H, O'Keeffe M, Yaghi OM (2008) High-throughput synthesis of zeolitic imidazolate frameworks and application to CO_2 capture. Science 319:939–943
17. Kevitiyagala N (2009) Carbon sequestration. Science 325:1644–1645
18. Yeh JT, Resnik KP, Rygle K, Pennline HW (2005) Semi-batch absorption and regeneration studies for CO_2 capture by aqueous ammonia. Fuel Process Technol 86:1533–1546
19. Horike S, Shimomura S, Kitagawa S (2009) Soft porous crystals. Nat Chem 1:695–704
20. Luo F, Wang M-S, Luo M-B, Sun G-M, Song Y-M, Lia P-X, Guo G-C (2012) Functionalizing the pore wall of chiral porous metal–organic frameworks by distinct –H, –OH, $–NH_2$, $–NO_2$, –COOH shutters showing selective adsorption of CO_2, tunable photoluminescence, and direct white-light emission. Chem Commun 48:5989–5991
21. Wang Z, Zheng B, Liu H, Lin X, Yu X, Yi P, Yun R (2013) High-capacity gas storage by a microporous oxalamide-functionalized NbO-type metal–organic framework. Cryst Growth Des 13:5001–5006
22. McDonald TM, D'Alessandro DM, Krishna R, Long JR (2011) Enhanced carbon dioxide capture upon incorporation of *N*,*N*′-dimethylethylenediamine in the metal–organic framework CuBTTri. Chem Sci 2:2022–2028
23. Haldar R, Bonakala S, Kanoo P, Balasubramanian S, Maji TK (2014) Two 3D metal–organic frameworks of Cd(II): modulation of structures and porous properties based on linker functionalities. CrystEngComm 16:4877–4885
24. Bhattacharya B, Haldar R, Maity DK, Maji TK, Ghoshal D (2015) Pillared-bilayer porous coordination polymers

of Zn(II): enhanced hydrophobicity of pore surface by changing the pillar functionality. CrystEngComm 17:3478–3486

25. Mowat JPS, Miller SR, Griffin JM, Seymour VR, Ashbrook SE, Thompson SP, Fairen-Jimenez D, Banu A-M, Duren T, Wright PA (2011) Structural chemistry, monoclinic-to-orthorhombic phase transition, and CO_2 adsorption behavior of the small pore scandium terephthalate, $Sc_2(O_2CC_6H_4CO_2)_3$, and its nitro- and amino-functionalized derivatives. Inorg Chem 50:10844–10858
26. Maity DK, Halder A, Bhattacharya B, Das A, Ghoshal D (2016) Selective CO_2 adsorption by nitro functionalized metal organic frameworks. Cryst Growth Des 16:1162–1167
27. Maity DK, Halder A, Ghosh S, Ghoshal D (2016) Azo functionalized 5-Nitro-1,3-benzenedicarboxylate based coordination polymers with different dimensionality and functionality. Cryst Growth Des 16:4793–4804
28. Dey R, Haldar R, Maji TK, Ghoshal D (2011) Three-dimensional robust porous coordination polymer with Schiff base site on the pore wall: synthesis, single-crystal-to-single-crystal reversibility, and selective CO_2 adsorption. Cryst Growth Des 11:3905–3911
29. Bhattacharya B, Haldar R, Dey R, Maji TK, Ghoshal D (2014) Porous coordination polymers based on functionalized Schiff base linkers: enhanced CO_2 uptake by pore surface modification. Dalton Trans 43:2272–2282
30. Bhattacharya B, Dey R, Pachfule P, Banerjee R, Ghoshal D (2013) Four 3D Cd(II)-based metal organic hybrids with different *N*,*N*′-donor spacers: syntheses, characterizations, and selective gas adsorption properties. Cryst Growth Des 13:731–739
31. Hijikata Y, Horike S, Sugimoto M, Inukai M, Fukushima T, Kitagawa S (2013) Pore design of two-dimensional coordination polymers toward selective adsorption. Inorg Chem 52:3634–3642
32. Halder A, Bhattacharya B, Dey R, Maity DK, Ghoshal D (2016) Reversible phase transformation in three dynamic mixed-ligand metal–organic frameworks: synthesis, structure, and sorption study. Cryst Growth Des 16:4783–4792
33. Carlucci L, Ciani G, Proserpio DM, Mitina TG, Blatov VA (2014) Entangled two dimensional coordination networks: a general survey. Chem Rev 114:7557–7580
34. Maity DK, Halder A, Pahari G, Haque F, Ghoshal D (2017) Hydrogen uptake by an inclined polycatenated dynamic metal–organic framework based aterial. Inorg Chem 56:713–716
35. Choi H-S, Suh MP (2009) Highly selective CO_2 capture in flexible 3D coordination polymer networks. Angew Chem Int Ed 48:6865–6869
36. Sharma MK, Senkovska I, Kaskel S, Bharadwaj PK (2011) Three-dimensional porous Cd(II) coordination polymer with large one-dimensional hexagonal channels: high pressure CH_4 and H_2 adsorption studies. Inorg Chem 50:539–544
37. Thallapally PK, Grateb JW, Motkuria RK (2012) Facile xenon capture and release at room temperature using a metal–organic framework: A comparison with activated charcoal. Chem Commun 48:347–349
38. Liu J, Strachan DM, Thallapally PK (2014) Enhanced noble gas adsorption in Ag@MOF-74Ni. Chem Commun 50:466–468
39. Fernandez CA, Liu J, Thallapally PK, Strachan DM (2012) Switching Kr/Xe selectivity with temperature in a metal–organic framework. J Am Chem Soc 134:9046–9049
40. Wang H, Yao K, Zhang Z, Jagiello J, Gong Q, Han Y, Li J (2014) The first example of commensurate adsorption of atomic gas in a MOF and effective separation of xenon from other noble gases. Chem Sci 5:620–624
41. Bardeen J (1947) Surface states and rectification at a metal semi-conductor contact. Phys Rev 71:717
42. Bhattacharya B, Layek A, Alam MM, Maity DK, Chakrabarti S, Ray PP, Ghoshal D (2014) Cd(II) based metal–organic framework behaving as a Schottky barrier diode. Chem Commun 50:7858–7861
43. Bhattacharya B, Maity DK, Layek A, Jahiruddin S, Halder A, Dey A, Ghosh S, Chowdhury C, Datta A, Ray PP, Ghoshal D (2016) Multifunctional mixed ligand metal organic frameworks: X-ray structure, adsorption, luminescence and electrical conductivity with theoretical correlation. CrystEngComm 18:5754–5763
44. Bhattacharya B, Dey R, Maity DK, Ghoshal D (2013) Formation of three new metal organic hybrids of Cd(II) with *N*,*N*′ donor spacer: an in situ perchlorate to chloride transformation. CrystEngComm 15:9457–9464
45. Maity DK, Bhattacharya B, Halder A, Ghoshal D (2015) Tuned synthesis of two coordination polymers of Cd(II) using substituted bent 3-pyridyl linker and succinate: structures and their applications in anion exchange and sorption properties. Dalton Trans 44:20999–21007

Dilip Kumar Maity completed his B.Sc. in 2009 and M.Sc. (inorganic chemistry specialisation) in 2011 from Ramakrishna Mission Residential College, Narendrapur, University of Calcutta, India. He is currently pursuing his Ph.D. in chemistry at the Department of Chemistry, Jadavpur University, India, under the supervision of Dr. Debajyoti Ghoshal. His research interests are synthesis and design of mixed-ligand metal–organic frameworks and their application in gas storage, selective gas adsorption and fuel cells.

Debajyoti Ghoshal obtained his Ph.D. in 2005 under the guidance of Prof. N. Ray Chaudhuri at the Indian Association for the Cultivation of Science, Kolkata, India. He worked with Prof. Dr. Herbert W. Roesky at the University of Göttingen, Germany, as an AvH fellow for his postdoctoral work. Presently, he is a faculty in the Department of Chemistry, Jadavpur University. His current research interests are crystal engineering and functional metal–organic frameworks (MOFs) with a special emphasis on selective gas storage by MOFs, conducting MOFs and framework-supported chemical transformation.